Organic Carbon Linkage with Soil Colloidal Phosphorus at Regional and Field Scales: Insights from Size Fractionation of Fine Particles

Li, Fayong; Zhang, Qian; Klumpp, Erwin; Bol, Roland; Nischwitz, Volker; Ge, Zhuang; Liang, Xinqiang

Environmental Science and Technology

DOI:
10.1021/acs.est.0c07709

Published: 04/05/2021

Peer reviewed version

Organic carbon linkage with soil colloidal phosphorus at regional and field scales: insights from size fractionation of fine particles

Fayong Li[1, 2#], Qian Zhang[3, 4#], Erwin Klumpp[3], Roland Bol[3, 5], Volker Nischwitz[6], Zhuang Ge[7], Xinqiang Liang[1*]

[1] Key Laboratory of Environment Remediation and Ecological Health, Ministry of Education, College of Environmental and Resources Sciences, Zhejiang University, Hangzhou 310058, China

[2] College of Water Resources and Architectural Engineering, Tarim University, Xinjiang 843300, China

[3] Institute of Bio- and Geosciences, Agrosphere (IBG-3), Forschungszentrum Jülich GmbH, 52425, Jülich, Germany

[4] Institute for Environmental Research, Biology 5, RWTH Aachen University, Worringerweg 1, 52074 Aachen, Germany

[5] School of Natural Sciences, Environment Centre Wales, Bangor University, Bangor, LL57 2UW, U.K.

[6] Central Institute for Engineering, Electronics and Analytics, Analytics (ZEA-3), Forschungszentrum Juelich, 52425 Juelich, Germany

[7] Northeast Key Laboratory of Conservation and Improvement of Cultivated Land (Shenyang), Ministry of Agriculture, Shenyang Agricultural University, Shenyang, Liaoning 110866, China

#These authors are co-first authors and contributed equally to this work

*Corresponding author: (liang410@zju.edu.cn; Tel & fax: 86-0571- 88982809)

ABSTRACT: Nano and colloidal particles (1–1000 nm) play important roles in phosphorus (P) migration and loss from agricultural soils; however, little is known about their relative distribution in arable crop soils under varying agricultural geo-landscapes at the regional scale. Surface soils (0–20 cm depth) were collected from 15 agricultural fields, including two sites with different carbon input strategies, in Zhejiang Province, China, and water-dispersible nano colloids (0.6–25 nm), fine colloids (25–160 nm), and medium colloids (160–500 nm) were separated and analyzed using Asymmetrical Flow Field Flow Fractionation (AF4) technique. Three levels of fine-colloidal P content (3583–6142, 859–2612, and 514–653 μg kg^{-1}) were identified at the regional scale. The nano colloidal fraction correlated with organic carbon (C_{org}) and calcium (Ca), and the fine colloidal fraction with C_{org}, silicon (Si), aluminum (Al), and iron (Fe). Significant linear relationships existed between colloidal P and C_{org}, Si, Al, Fe, Ca, and for nano-colloidal P with Ca. The organic carbon controlled colloidal P saturation, which in turn affected the P carrier ability of colloids. Field-scale organic carbon inputs did not change the overall morphological trends in size fractions of water dispersible colloids. However, they significantly affected the peak concentration in each of the nano-, fine- and medium-colloidal P fractions. Application of chemical fertilizer with carbon-based solid manure and/or modified biochar reduced the soil nano-, fine- and medium-colloidal P content by 30–40%; however, application of chemical fertilizer with biogas slurry boosted colloidal P formation. This study provides a deep and novel understanding of the forms and composition of colloidal P in agricultural soils and highlights their spatial regulation by soil characteristics and carbon inputs.

Keywords: organic carbon; nano-colloidal phosphorus; colloidal phosphorus; Asymmetric Flow Field-Flow Fractionation; biochar; regional scale; field scale

Table of Contents (TOC) Art:

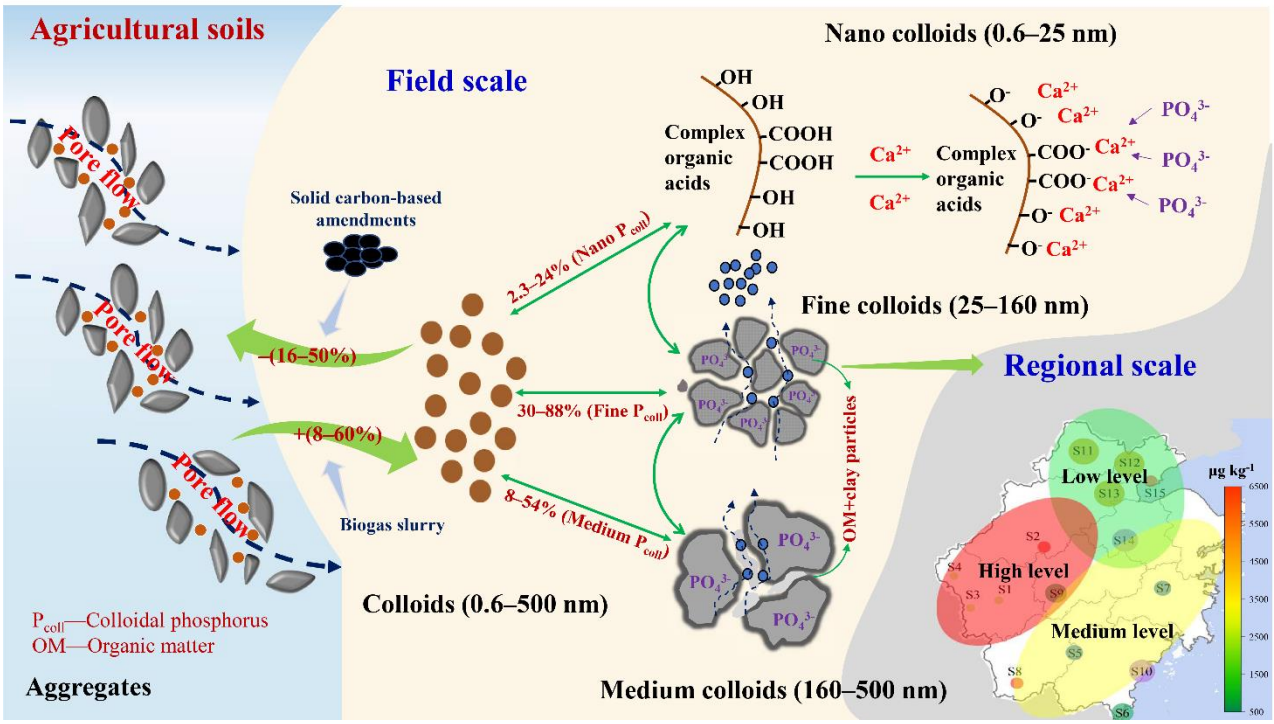

INTRODUCTION

Loss of soil phosphorus (P) from agricultural fields has long been a global challenge, and is one of the main factors responsible for the eutrophication of rivers and lakes in southern China[1,2]. However, the formation, distribution, and migration mechanisms of P in agricultural soils remain inadequately understood, which presents great difficulties in source control mitigation where P is present as a diffuse and non-point pollution source[3]. Previous studies suggest that the majority of P in soil exists as larger-sized particulate and conventionally dissolved P, which are usually distinguished using a 0.45 μm filter membrane[4,5] However, this consideration neglects the important role of colloidal P (~1–1000 nm) and its subfraction nano-colloidal P (~1–100 nm) in the process of soil P transport. In fact, colloidal P forms have special colloid-chemical properties[6,7], which are fundamentally different from that of truly dissolved P. In general, colloidal size fractions like nano colloids (~1–100 nm), fine colloids (~100–200 nm), and medium colloids (~200–500 nm) have a large specific surface area and are rich in charge density, and, thus, they can immobilize P and other compounds[8,9]. The colloidal P can potentially migrates faster than truly dissolved P due to the spatial exclusion and electrostatic repulsion of the soil matrix[10]. Moreover, some studies have found that the P molecules carried by colloids with low bioavailability and small particle size enhance migration ability and contribute to the transport of soil P to external water bodies[11–13]. Overall, the migration and transformation of colloidal P in agricultural soil systems is of crucial environmental and ecological significance.

Related studies in acid forest river systems have indicated that organic carbon (C_{org}), iron (Fe), and aluminum (Al) may be the main binding elements of nano-, fine- and medium-colloidal P, and

66 that the elemental composition may vary with the specific location within or between rivers[14–15].
67 However, detailed colloidal P fluxes remain almost blind spots in some areas of ecosystem research[16].
68 In agricultural systems, colloidal carriers may be affected by farm management practices, such as
69 irrigation, fertilization, and land-use types[12,17]. Compared to forest soils, agricultural soils usually
70 have lower organic matter, higher inorganic mineral contents, and relatively stable seasonal input
71 and outputs[18]. Therefore, the composition and morphology of the colloids in agricultural soils may
72 be very different from those in natural ecosystems, e.g., forest and steppe soils. The majority of
73 previous research on colloidal P in agricultural systems has focused on the whole colloidal size range
74 (1–1000 nm) and single, specific farm types[17], and only few studies have separated nano-, fine- and
75 medium-colloidal P[19,20]. The rarest studies are those that also provide specific nutrient compositions
76 of colloidal particle size ranges[21,22]. The emergence of the Asymmetrical Flow Field Flow
77 Fractionation (AF4) technique enables us to separate and study nano-, fine- and medium-colloidal
78 P[23]. As an important advantage of this technique, crude extracts of soil water dispersible colloids
79 can be analyzed with the only requirement that the upper particle size is limited to about 500 nm by
80 centrifugation. The composition of nano-, fine- and medium-colloidal P in stream waters and soils
81 has been explored using this technique[24,20,25,26].

82 Input of carbon-based fertilizers directly affects the forms, composition, and loss of P in
83 agricultural soils[27,28]. Organic fertilizer (manures) usually contains a large amount of organic P,
84 which may increase the soil P level after being applied to the soil[29]. However, it may also reduce the
85 release of soluble P and improve soil bacteria activity compared with chemical fertilizers[2,30].
86 Carbon-based biochar has recently been recommended as an amendment that effectively improves

soil physical and chemical conditions and increases crop productivity[31–32]. However, biochar contains a large amount of soluble P, which may increase the loss of soil P once applied to the soil[33]. Conversely, it is rich in pore structures, specific surface area, and functional groups, which may have the potential to immobilize soil P[33,34]. However, regardless of the type of fertilization, organic carbon input will participate in the formation of soil colloidal particles after entering the soil, whereby some may be adsorbed by the colloids, and some may have colloidal properties (i.e., high molecular mass organic acids). At present, there are very few reports on the elemental compositions and morphologies of soil colloidal P under different carbon input strategies.

Therefore, we collected soil samples covering typical agricultural ecosystems from 15 sites throughout Zhejiang Province, China, to explore the influence of organic carbon and other soil parameters on nano-, fine- and medium-colloidal P at the regional scale. At the field scale, two experimental stations were established to evaluate the effects of different carbon input strategies on the soil P forms, content, and loss potential. Soil samples were analyzed using AF4 coupled to inductively coupled plasma-mass spectrometry (ICP–MS) and to an online organic carbon detector (OCD). We hypothesized that, due to different formation mechanisms: i) At the regional scale, specific distribution patterns of nano-, fine- and medium-colloidal P occur under different land-use types, and organic carbon affects the ability of colloids and nanoparticles to bind P; ii) at the field scale, chemical fertilizer will increase soil nano-, fine- and medium-colloidal P concentrations; however, carbon inputs (including organic fertilizer and biogas slurry, with or without modified biochar) will reduce the soil nano-colloidal and fine/medium-colloidal P contents.

■ MATERIALS AND METHODS

Site description and soil sampling. Soil samples were taken from 15 representative sites (H1–H5, M1–M5, and L1–L5) with different land-use types in Zhejiang Province (Figure S1), China, which included 6 agricultural planting types with conventional fertilization regimes (Tables S1 and S2), which were almost evenly distributed in the county-level administrative area of the region (1,055,00 km^2, Figure S1). In each sampling site, three representative fields (three replicates) of the same crop type were selected, and 10-kg topsoil samples (0–20 cm depth) were randomly collected from 10–15 points of each field without regard to soil horizons using S-shaped sampling method[35] and then mixed to prepare a representative sample of the whole field. Samples were air-dried and divided into two portions: One portion was ground through a 0.154-mm sieve for determining the basic physical and chemical properties, and the other portion was carefully broken into small pieces by hand and passed through an 8-mm sieve for separation of water-dispersible colloids (WDC) and determination of colloidal fractions. All the soil samples were stored in sealed plastic bags and kept at 4°C before analysis. Detailed descriptions of sites and soils are shown in Table S1.

In addition, two experimental crop rotation field stations were established as part of the study (Figure S1), i.e., in Site 1 (double-season rice) and Site 2 (rice-wheat rotation). Three treatments with the same P application rate and a control (CK) were applied at each site. The P application rates were 68.8 kg P ha^{-1} per year (two seasons) at Site 1 and 103.2 kg P ha^{-1} per year (two seasons) at Site 2. The treatments in Site 1 were: a) Control without fertilization (CK), b) Conventional fertilization (chemical fertilizer, CF), c) Chemical fertilizer + organic fertilizer (sheep manure) (OF), and d) Chemical fertilizer + organic fertilizer + modified rice straw biochar (OFSB). The treatments in Site 2 were: e) Control without fertilization (CK), f) conventional fertilization (CF), g) Chemical

fertilizer + biogas slurry (BS), and h) Chemical fertilizer + biogas slurry + modified rice straw biochar (BSSB). Each treatment was repeated three times with a total of 12 completely random plots (33.3 m^2 per each). Physicochemical properties of modified biochar, organic fertilizer, and biogas slurry are shown in Table S3. The specific nutrient contents of fertilizers and the fertilization schedule are shown in Tables S4 and S5, respectively. Five soil samples from the 0–20 cm soil layer in each plot were randomly collected after harvesting in the second season and were mixed into a 5-kg sample, transported to the laboratory, air-dried, and again divided into two equal portions (i.e., as for all main site samples). One portion was ground through a 0.154-mm sieve to determine basic physical and chemical properties. The other portion was carefully broken into small pieces by hand and passed through an 8-mm sieve for separation of WDC.

Soil physical and chemical parameters. Soil particle size distribution was determined using the hydraulic method according to the international soil texture classification[36]. Soil pH was determined using a glass electrode pH meter (PHS-3C, Shanghai) at a solid-to-liquid ratio of 1:5. Soil cation exchange capacity (CEC) was determined using ammonium acetate (12.5 mL 1 M NH_4OAc, 2.5 g soil)[37]. Samples were digested with H_2SO_4-$HClO_4$, and the total P contents were determined using molybdenum blue colorimetric method[38]. Soil total carbon (TC) and total nitrogen (TN) were measured using an element analyzer (Elementar, Vario MAX CNS, Germany). The bioavailable fraction of Fe, Al, and Ca was determined using an Inductively Coupled Plasma-Mass Spectrometer (ICP-MS; Agilent 7500, Agilent Technologies, Japan) after extraction by 0.2 mol L^{-1} oxalic acid (2.5 g soil, 50 mL oxalic acid)[39]. Soil available P (Olsen P) was extracted with 0.5 M $NaHCO_3$ (pH 8.5)[40] and analyzed using molybdenum blue colorimetry.

Water dispersible colloids extraction. The water-dispersible soil colloids were extracted by the method of Sequaris and Lewandowski [41], which avoids the destruction of small aggregates in soil[25], and mainly includes two procedures of shaking and sedimentation at a water to soil mass ratio of 1 to 8 to obtain WDC suspension. All samples were extracted and analyzed in triplicate. In brief, 10 g soil subsamples (d < 8 mm) were mixed with 20 mL deionized water and shaken on a horizontal shaker at 150 rpm for 6.5 h. The suspension was then diluted four times with deionized water and left to stand to allow sedimentation (approximately 6 min, according to Stokes' law, particle density was assumed as 1.5 g cm^{-3}) to remove the particles > 20 μm[10,42]. Then, the supernatant was transferred into a 25-mL centrifuge tube, and the suspension (< 20 μm) was centrifuged at 4000 rpm for approximately 7 min. The centrifugation time was calculated according to Hathaway (1956) to obtain WDC with a particle size of < 500 nm in the supernatant[43,44]. Irrigation experiments with undisturbed mesocosm soil columns demonstrated that the leached colloids had a maximum size of 400 nm[26]. For additional details see supplementary information (section S1). In addition, dynamic light scattering (DLS) measurements (Malvern Nano-ZS, Malvern Panalytical, UK) were performed on the separated WDC samples to verify the effectiveness of the size fractionation, and the z-average of diameter was calculated based on the intensity distribution (Table S6)[43,19].

The truly dissolved elemental fractions were determined by ultrafiltration using a molecular weight cut off of 3 kDa (Millipore, USA). 15 mL of WDC suspension were centrifuged at 4000 g for 15 min. The permeate was collected and analyzed by ICP-MS and OCD for P, Fe, Al, Si, Ca, Mg and organic carbon.

Asymmetric Flow Field Flow Fractionation

171 Size resolved elemental characterization of the colloidal fractions in the extracted WDCs was
172 achieved by AF4 (AF2000, Postnova Analytics, Landsberg, Germany) using a 1 kDa PES membrane,
173 1 mL injection volume, 20 min focusing time and a separation time of 91 min including a cross flow
174 gradient from 2.5 mL min^{-1} down to zero. The AF4 was coupled online to a UV-vis detector
175 (Postnova Analytics), a DLS detector (Malvern Nano-ZS, Malvern Panalytical, UK) and a C_{org}
176 detector (OCD; DOC laboratory Dr. Huber, Germany) for quantification of the particulate organic
177 carbon using multipoint external calibration and determination of the particle size. In parallel, the
178 same AF4 method was run with ICP-MS detection (Agilent 7500, Agilent Technologies, Japan) for
179 quantification of the particulate elemental concentrations monitoring ^{31}P, ^{56}Fe, ^{27}Al, ^{28}Si, ^{44}Ca and
180 ^{24}Mg using He collision cell mode. A post channel calibration approach was applied using Rh as the
181 internal standard which was developed and validated in our previous work[45,46]. Latex particles were
182 analyzed with the same AF4 method as size markers for the obtained colloidal fractions (Figure S2).
183 Further experimental details are given in the supporting information (section S2, Table S7 and Table
184 S8).

185 **Colloidal Phosphorus Saturation.** Similar to the definition of soil P saturation (DPS)[47], the
186 colloidal P saturation (DPS_{coll}) was used to assess the P adsorption capacity of soil colloids at 15
187 sites in Zhejiang Province. The DPS_{coll} was calculated using the following formula:

188 $$DPS_{coll} = \frac{P_{coll}}{Fe_{coll} + Al_{coll}} \times 100\%$$

189 where Fe_{coll}, Al_{coll}, and P_{coll} denote the Fe, Al, and P contents in the colloid, respectively, and the unit
190 of the Fe_{coll}, Al_{coll}, and P_{coll} is mmol kg^{-1}.

191 **Statistical Analysis.** Statistical analysis was performed using SPSS statistical software

192 package (SPSS Inc. Chicago, USA). A least significant difference (LSD) test at $P = 0.05$ level was
193 used to determine significant differences among the results of different fertilization treatments.
194 Origin 20.0 software (OriginLab Corp., US) was used for graphical processing. Pearson correlation
195 analysis and linear fitting were used to identify the relationships between nano-, fine- and medium-
196 colloidal P, and other colloidal and soil parameters.

197 ## ■ RESULTS

198 **Soil colloidal composition under varying agricultural geo-landscapes.** The fractograms
199 indicated that all 15 soil samples consisted of 2 or 3 size fractions as observed by the monitored
200 elemental peaks with similar elution times between samples (Figure 1). The first peak contained the
201 smaller nano colloids (approximately 0.6–25 nm; lower limit calculated from the membrane pore
202 size of 1 kDa); the second peak was assigned to larger nano colloids and fine colloids (approximately
203 25–160 nm, fine colloidal fraction); the third peak (after release of the cross flow) was related to
204 medium colloids (approximately 160–500 nm). In all H, all M and the L1 soils, all three fractions
205 were observed, and generally dominated by the fine colloidal fraction except for L1. However, in
206 L2–L5, only the first and third fraction was detected.

207 The soil colloidal P (0.6–500 nm) can be divided into three groups: high (H1–H5, 3583–6142
208 μg kg^{-1}), medium (M1–M5, 859–2612 μg kg^{-1}), and low (L1–L5, 514–653 μg kg^{-1}) (Figure 2, Table
209 1). The medium and high-level groups originated from the Basins and Mountains of Central and
210 Southeast, which were characterized by very low P contents in the nano- and medium-colloidal size
211 fractions, however, contained high amount of P in the fine-colloidal fraction. The fine-colloidal P
212 content of the high-level group accounted for 77–89% of the total determined colloidal P content

213 (Figure 2, Table 1). Peaks of fractograms were much less clear for northern plains soils, which
214 comprised the low-level colloidal P group (Figure 2). The fine- and medium-colloidal P here only
215 accounted for 28–39% and 35–53%, respectively, of the total colloidal P measured (Table 1).

216 In general, C_{org}, Si, Al, and Fe were the main constituent elements of soil fine and medium
217 colloidal fractions, while the C_{org} and Ca contents were most abundant of the monitored elements in
218 the soil nano colloidal fraction (Figure S3, Table 2). When comparing different colloidal size
219 fractions, the mean contents of C_{org}, Si, Al, and Fe (447, 164, 56.2 and 19.8 mg kg^{-1}, respectively),
220 were much higher than the mean Ca concentration (1.8 mg kg^{-1}) in the fine and medium colloidal
221 size (Figure S3, Table 2). However, in the nano colloidal fraction C_{org} and Ca were more abundant
222 with mean contents of 150.7 and 0.7 mg kg^{-1} compared to the rather low mean contents of Fe and
223 Al of 0.2 mg kg^{-1} and 0.5 mg kg^{-1}, respectively (Figure S3).

224

225 **Linkages of colloidal P with organic carbon at regional scale.** Colloidal Al, Fe, Ca, Si, and
226 C_{org} compositions were significantly correlated with colloidal P ($P < 0.05$). However, the fitting
227 results varied with the colloidal size fractions. For the nano colloidal fraction, only Ca and P
228 displayed a linear relationship (Figure 3). However, linear relationships were found between P and
229 C_{org}, Si, Al, Fe, and Ca in the fine colloidal fraction. In the medium colloidal fraction, there were
230 linear relationships between P and C_{org}, Si, Al, and Fe, with the strongest relationship between P and
231 Al (Figure 3).

232 The P saturation in the colloids showed that the L1–L5 had higher soil DPS_{coll} levels in the total
233 fractions, with a mean of ca. 20%, whereas it was only 1% in H1–H5 and M1–M5 (Table 1). In

addition, our analysis showed that DPS_{coll} was closely related to colloidal C_{org} (Figure 4). When the C_{org} concentration was < 200 mg kg^{-1}, the DPS_{coll} decreased sharply with the increase in the C_{org} content, and when it exceeded 200 mg kg^{-1}, DPS_{coll} decreased gently with the increase of C_{org}, and the scatter plot after log-transformation showed a negative correlation between C_{org} and DPS_{coll} (Figure 4).

Soil colloidal composition under different organic amendments input. Carbon-based fertilizer inputs did not affect the fractogram shapes of nano, fine, and medium colloids in the two soils (Figures S4 and S5), and did not change the magnitude (medium level) of the colloidal P distribution at the regional scale. The above assigned three size fractions were present in all treatments. However, compared with the control, all treatments showed a (slight) increase in the peak value (concentration), except for OFSB in which it decreased. Compared with CF, the OF treatment mainly caused a significant increase of the C_{org} content of the nano colloidal fraction, but Al, Fe, and Ca contents decreased in the fine colloids (Table S9, Figure S6). The BS treatment significantly increased the C_{org} concentration in both nano and fine colloidal fractions ($P < 0.05$). Furthermore, OFBS and BSSB significantly decreased the Al, Fe, and Ca contents in colloidal fractions ($P < 0.05$).

Compared with CF at Site 1, the OF and OFSB treatments reduced the soil colloidal P content (0.6–500 nm) by 33% and 43%, respectively, while at Site 2, BS increased colloidal P by 30% and BSSB reduced colloidal P by 45% (Figure 5). In comparison with CF, the treatments of OF, OFBS, and BSSB significantly reduced the concentration of fine colloidal P ($P < 0.05$), but had little effect

on nano colloidal P. However, the nano-colloidal P concentration of BS treatment was 50% higher than that of CF, while the fine-colloidal P concentration of BS were 74%, 39%, and 178% higher than those of CK, CF, and BSSB, respectively. In the medium colloidal fraction, no significant differences of P content were detected between CK, CF, and OF/BS, however, in OFBS and BSSB treatments, it was significantly lower than all other treatments. The truly dissolved P content of the two soils significantly decreased after organic fertilizers application when compared to CF ($P < 0.05$), while the ratio between fine colloidal P and the truly dissolved P was higher in the two soils with modified biochar (Figure S7).

■ DISCUSSION

Colloidal P formation as revealed by regional-scaled observation. In this study, 2 or 3 colloidal fractions were found in 15 soils, which is similar to the findings in other soils or streams[20,26,43]. However，we found two distinct linkages of organic matter with the nano-colloidal P and fine- and medium-colloidal P, respectively. Nano colloidal P is correlated with organic carbon and Ca and most likely forming a complex of C_{org}-Ca-P, while fine colloidal and medium colloidal P is correlated with clay mineral elements and likely to form a complex of C_{org}-clay-P.

Colloids (< 450 nm) extracted from soil or stream water usually contain nano-sized organic matter (complex organic acids) in the size range of 1–5 nm[19]. Moreover, some macromolecular degradation products and excretes (<100 nm) by microorganisms within soil, mainly comprising of protein, DNA, and fat as well as extracellular polymeric substance (EPS), co-exist with P, which was revealed by the high concentrations of P-monoesters and P-diesters in the WDC extract identified by NMR (Figure S8, Table S10). In most soils, nano-colloidal Fe and Al were present at

non-detectable levels, while Ca was present in significant amount along with organic carbon. This is different from the finding[19] by Jiang et al, 2015 that implied the binding mechanism of organic matter and amorphous Fe or Al oxides in the nano colloidal fraction (<20 nm) of an acidic soil. However, a recent study showed that binary humic acid (HA)-Ca complexes could incorporate P by forming ternary HA-Ca-P complexes[48], and the P may also be bound in nano-colloidal minerals of apatite[49,50]. Furthermore, in calcareous soils, Ca^{2+} ions presumably bridged organic P and nano colloidal negatively charged organic substances with carboxyl or phenolic groups[42,51,52]. Therefore, we assume that nano colloids are dominated by organic compounds, and that their small-sized acid moieties may form stable nanoparticles through the bridging of Ca^{2+} ions. This is also supported by a strongly positive correlation with nano-colloidal Ca and P, but non-significant correlations with nano-colloidal Fe, Al, or Si (Figure 3). However, the fact that there were little differences between the C_{org} content in nano colloids of the soils, and C_{org}/P and Ca/P were basically fixed at approximately 4000:1 and 4:1, respectively (Table 2 and S10), may indicate that the binding capacity of P to nano colloids was limited.

The fine colloidal fraction with the highest intensity of the three separated size fractions in most soils (H1–H5 and M1–M5) contains large amounts of C_{org}, Si, Al, and Fe, and this size fraction is usually formed from stable organic-inorganic composite colloids consisting of clay minerals, Fe/Al (hydr)oxides and organic matter[19,53]. This was revealed by the fixed molar ratio of Si/Al (1:0.5) elements in the colloids (Table S11), which was consistent with the composition of 2:1 clay minerals[19,54,55], and the fact that the soil clay minerals in the Zhejiang area contains more muscovite and montmorillonite (Figure S9)[56]. Considering the relatively constant Fe/Si molar ratio

297 (approximately 0.1:1; Table S11), the clay minerals in this area may have the fixed ratio of
298 isomorphic substitution between Fe and Al[57], and/or Fe oxides form complexes with clay minerals
299 and organic matter, respectively. The medium colloidal fraction with a lower intensity, represented
300 the larger WDC, but may have included small aggregates of nano and fine colloids[19] and occasional
301 residual particles of sizes > 500 nm. In contrast to H1–H5 and M1–M5 soils, the fine colloidal
302 fraction of L1–L5 soils is missing, which may be related to the lower clay content of these soils
303 (Table S1). Some studies reported that the soil colloid content is closely related to the clay mineral
304 content[58,59], which presumably immobilizes the P in the soil through adsorption, ligand exchange,
305 and precipitation[19,60–61]. The fine-colloidal P dominated by C_{org}, Si, Fe, and Al, accounted for 80%
306 of the total colloidal P for H1–H5 and M1–M5 and 36% of total colloidal P for L1–L5. Note, Ca^{2+}
307 may also participate in the fine colloid formation process, connecting colloids and organic matter[42,62].
308 In addition, Ca^{2+} may play an important role in bridging inorganic P and organic P on clay minerals
309 accompanied by organic matter[45].

310 The P saturation in the colloids showed that the L1–L5 had significantly higher soil DPS_{coll}
311 levels than H1–H5 and M1–M5 (Table 1). Furthermore, there was a negative correlation between
312 the DPS_{coll} and C_{org} concentrations (Figure 4). Some studies also confirmed that when the surface
313 adsorption sites of soil are occupied by a large amount of organic substances, the adsorption capacity
314 of clay particles for phosphate ions will be weakened[63–64]. The organic carbon compounds with
315 competitive inhibition of P sorption are usually derived from low molecular weight organic acids
316 (LOAs), humic and fulvic acids, and organic leachates[65]. Therefore, the degree of P saturation in
317 fine and medium colloids can directly reflect the amount of soil P carried by the colloids which can

318 be used in the future to predict the P retention capacity of soil colloids and the risk of P loss. It is
319 worth noting that in nano colloids fraction, the adsorption mechanism of P was not related to Fe and
320 Al, but rather to the complexation of Ca and organic matter. Therefore, DPS_{coll} cannot be simply
321 used for the prediction of nano-colloidal P in the soils studied.

322 Colloidal P in the fractograms of the agricultural soil colloids revealed spatial distribution
323 characteristics at the regional scale (Table 1). This also may be subject to the differences in soil
324 mineralogy and organic C storage. A study in the subtropical forests found that soil organic C was
325 highly correlated with P sorption index[66], and many organic P compounds sorb strongly to positively
326 charged mineral surfaces of amorphous Al and Fe oxide and the edge of clay minerals[67]. The
327 subtropical monsoon affected humid climate zone in the middle and southern Zhejiang where the
328 soil is rich in iron and aluminum and lower in C storage (Table S1)[56], resulting in the existence of a
329 high-medium level group of colloidal P. Soils on the Northern Plain usually have lower
330 aluminization and obvious accretion layers[56] and show a higher C storage and clay content (Table
331 S1), resulting in the low level group of colloidal P. This pattern assignment also basically proves our
332 first hypothesis that specific distribution patterns of colloidal P occur at regional scale. However, in
333 fact, the terrain topography in Zhejiang Province is complicated[56], and the current classification of
334 colloidal P fractions in this region is therefore still relatively coarse. Note, in view of the high
335 instrumental and time effort of the AF4 technology with ICP-MS detection for testing a large number
336 of samples, an initial set of 15 samples (3 repetitions each) was investigated in detail in this study to
337 achieve a basic characterization at the regional scale. A further study in the future is needed to
338 increase the sampling site density and evaluate the colloidal P distribution pattern in higher spatial

and possibly even temporal resolution at the regional scale.

Effects of organic fertilizer inputs on soil colloidal P. Our study found that 2 years of differential fertilization had no significant effect on the fractogram shape (i.e., magnitude and composition) of nano- and fine-colloidal sized particles isolated from two soils. Therefore, we conclude that the soil textures and the contents of the particulate matrix elements (i.e., C_{org}, Fe, Al, Si, Ca) affect the composition, distribution, and morphology of soil colloidal fractions, while the difference in the type of fertilization and carbon inputs affects the concentration of compounds (i.e., P) adsorbed by colloids. However, the ability of colloids in different soils to carry P has been determined by soil conditions, which is supported by the concept of DPS_{coll} proposed above. Therefore, the first step to investigate the colloidal loss potential of a special type of soil is to understand its organic and mineral phase composition. This is an important prerequisite for formulating a P management strategy. Understanding this premise is of great significance to the management of P loss in the agricultural field at different regional scale.

Indeed, fertilization regimes significantly affected the soil nano-colloidal P and fine-colloidal P concentrations in a particular type of soil. Specifically, compared with the control, the application of chemical fertilizer enhanced the P saturation of fine colloids by increasing the phosphate concentration, and boosted the nano-colloidal and fine-colloidal P contents in the soil. The strong correlation between the truly dissolved P or available P and colloidal P further confirmed the occurrence of that process (Figure S10). Compared with CF, when organic fertilizer replaced 30% of the chemical P, the colloidal P content significantly decreased. This was mainly due to the increase

of organic matter, which sheltered the colloidal adsorption sites[63,64], and limited the chances of the phosphate ions binding to colloids through adsorption, resulting in the reduction of the amount of colloidal P. We further found that compared with the application of chemical fertilizers, organic fertilizer and biochar applications increased the concentration of C_{org} in the soil colloids, but decreased the concentrations of Fe and Al (Table S10). A study of a loam soil with long-term application of poultry manure found that P was more likely to be associated with Ca than Fe or Al[68] and resulted in the conversion of relatively soluble Ca-P into more colloidal crystal phases. However, when applying biogas slurry instead of 30% chemical P, the amounts of nano-colloidal and fine colloidal P in the soil increased significantly (Figure 5). This may be due to the biogas slurry itself containing a large amount of organic colloidal P, which is bound to clay colloids or exist in the nano P form once entering the soil[29]. Compared with CF, OF, and BS, the application of modified biochar significantly reduced the amount of colloidal P in the soil. The two explanations for this are: 1) P adsorption on biochar[33], and 2) the modified biochar promotes the formation of soil aggregates[69]. Overall, more systematic field experiments including runoff and leaching losses are warranted to investigate and verify the effect of fertilization on the morphology and migration of colloidal P.

■ ASSOCIATED CONTENT

Supporting Information

Sections S1-S3; Figures S1–S10; Tables S1–S11

■ AUTHOR INFORMATION

Corresponding Author

Xinqiang Liang − Key Laboratory of Environment Remediation and Ecological Health, Ministry of Education, College of Environmental and Resources Sciences, Zhejiang University, Hangzhou 310058, China. https://orcid.org/0000-0002-3521-9761

Tel & fax: 86-0571- 88982809

Email : liang410@zju.edu.cn

Authors

Fayong Li − Key Laboratory of Environment Remediation and Ecological Health, Ministry of Education, College of Environmental and Resources Sciences, Zhejiang University, Hangzhou 310058, China. https://orcid.org/0000-0002-7893-9451

Qian Zhang − Institute of Bio- and Geosciences, Agrosphere (IBG-3), Forschungszentrum Jülich GmbH, 52425, Jülich, Germany; Institute for Environmental Research, Biology 5, RWTH Aachen University, Worringerweg 1, 52074 Aachen, Germany.

Erwin Klumpp − Institute of Bio- and Geosciences, Agrosphere (IBG-3), Forschungszentrum Jülich GmbH, 52425, Jülich, Germany. https://orcid.org/0000-0002-4810-9414

Roland Bol − Institute of Bio- and Geosciences, Agrosphere (IBG-3), Forschungszentrum Jülich GmbH, 52425, Jülich, Germany; School of Natural Sciences, Environment Centre Wales, Bangor University, Bangor, LL57 2UW, U.K. https://orcid.org/0000-0003-3015-7706

Volker Nischwitz − Central Institute for Engineering, Electronics and Analytics, Analytics (ZEA-3), Forschungszentrum Juelich, 52425 Juelich, Germany. https://orcid.org/0000-0002-9261-3124

Zhuang Ge − Northeast Key Laboratory of Conservation and Improvement of Cultivated Land (Shenyang), Ministry of Agriculture, Shenyang Agricultural University, Shenyang, Liaoning 110866, China.

Notes

The authors declare no competing financial interest.

■ ACKNOWLEDGEMENTS

We are grateful for grants from National Natural Science Foundation of China (41522108;22076163); National Key Science and Technology Project: Water Pollution Control and Treatment (2018ZX07208009); Natural Science Foundation of Zhejiang Province (LR16B070001). We thank China Scholarship Council for providing scholarships to the students in this study.

REFFERENCES

(1) He, S.; Li, F. Y.; Liang, X. Q.; Li, H.; Wang, S.; Jin, Y. B.; Liu, B. Y.; Tian, G. M. Window Phase Analysis of Nutrient Losses from a Typical Rice-Planting Area in the Yangtze River Delta Region of China. *Environ. Sci. Eur.* **2020**, *32* (1), 1–12. https://doi.org/10.1186/s12302-020-0291-0.

(2) Liang, X.; Jin, Y.; He, M.; Liu, Y.; Hua, G.; Wang, S.; Tian, G. Composition of Phosphorus Species and Phosphatase Activities in a Paddy Soil Treated with Manure at Varying Rates.

Agric. Ecosyst. Environ. **2017**, *237*, 173–180. https://doi.org/10.1016/j.agee.2016.12.033.

(3) Bol, R.; Gruau, G.; Mellander, P. E.; Dupas, R.; Bechmann, M.; Skarbøvik, E.; Bieroza, M.; Djodjic, F.; Glendell, M.; Jordan, P.; Van der Grift, B.; Rode, M.; Smolders, E.; Verbeeck, M.; Gu, S.; Klumpp, E.; Pohle, I.; Fresne, M.; Gascuel-Odoux, C. Challenges of Reducing Phosphorus Based Water Eutrophication in the Agricultural Landscapes of Northwest Europe. *Front. Mar. Sci.* **2018**, *5* (AUG), 276. https://doi.org/10.3389/fmars.2018.00276.

(4) Solórzano, L.; Sharp, J. H. Determination of Total Dissolved Phosphorus and Particulate Phosphorus in Natural Waters. *Limnol. Oceanogr.* **1980**, *25* (4), 754–758. https://doi.org/10.4319/lo.1980.25.4.0754.

(5) Hens, M.; Merckx, R. The Role of Colloidal Particles in the Speciation and Analysis of "Dissolved" Phosphorus. *Water Res.* **2002**, *36* (6), 1483–1492. https://doi.org/10.1016/S0043-1354(01)00349-9.

(6) Klitzke, S.; Lang, F.; Kaupenjohann, M. Increasing PH Releases Colloidal Lead in a Highly Contaminated Forest Soil. *Eur. J. Soil Sci.* **2008**, *59* (2), 265–273. https://doi.org/10.1111/j.1365-2389.2007.00997.x.

(7) Ran, Y.; Fu, J. M.; Sheng, G. Y.; Beckett, R.; Hart, B. T. Fractionation and Composition of Colloidal and Suspended Particulate Materials in Rivers. *Chemosphere* **2000**, *41* (1–2), 33–43. https://doi.org/10.1016/S0045-6535(99)00387-2.

(8) Hartland, A.; Lead, J. R.; Slaveykova, V. I.; O´Carroll, D.; Valsami-Jones, E. The Environmental Significance of Natural Nanoparticles | Learn Science at Scitable. *Nat. Educ. Knowl.* **2013**, *4* (8), 7.

(9) Qafoku, N. P. Terrestrial Nanoparticles and Their Controls on Soil-/Geo-Processes and Reactions. *Adv. Agron.* **2010**, *107* (C), 33–91. https://doi.org/10.1016/S0065-2113(10)07002-1.

(10) Henderson, R.; Kabengi, N.; Mantripragada, N.; Cabrera, M.; Hassan, S.; Thompson, A. Anoxia-Induced Release of Colloid- and Nanoparticle-Bound Phosphorus in Grassland Soils. *Environ. Sci. Technol.* **2012**, *46* (21), 11727–11734. https://doi.org/10.1021/es302395r.

(11) Jiang, X.; Livi, K. J. T.; Arenberg, M. R.; Chen, A.; Chen, K. yue; Gentry, L.; Li, Z.; Xu, S.; Arai, Y. High Flow Event Induced the Subsurface Transport of Particulate Phosphorus and Its Speciation in Agricultural Tile Drainage System. *Chemosphere* **2021**, *263*, 128147. https://doi.org/10.1016/j.chemosphere.2020.128147.

(12) Li, F. Y.; Liang, X. Q.; Liu, Z. W.; Tian, G. M. No-till with Straw Return Retains Soil Total P While Reducing Loss Potential of Soil Colloidal P in Rice-Fallow Systems. *Agric. Ecosyst. Environ.* **2019**, *286*, 106653. https://doi.org/10.1016/j.agee.2019.106653.

(13) Kaplan, D. I.; Bertsch, P. M.; Adriano, D. C.; Miller, W. P. Soil-Borne Mobile Colloids as Influenced by Water Flow and Organic Carbon. *Environ. Sci. Technol.* **1993**, *27* (6), 1193–1200. https://doi.org/10.1021/es00043a021.

(14) Baken, S.; Moens, C.; van der Grift, B.; Smolders, E. Phosphate Binding by Natural Iron-Rich Colloids in Streams. *Water Res.* **2016**, *98*, 326–333. https://doi.org/10.1016/j.watres.2016.04.032.

(15) Gottselig, N.; Bol, R.; Nischwitz, V.; Vereecken, H.; Amelung, W.; Klumpp, E. Distribution of Phosphorus-Containing Fine Colloids and Nanoparticles in Stream Water of a Forest

Catchment. *Vadose Zo. J.* **2014**, *13* (7), vzj2014.01.0005. https://doi.org/10.2136/vzj2014.01.0005.

(16) Bol, R.; Julich, D.; Brödlin, D.; Siemens, J.; Kaiser, K.; Dippold, M. A.; Spielvogel, S.; Zilla, T.; Mewes, D.; von Blanckenburg, F.; Puhlmann, H.; Holzmann, S.; Weiler, M.; Amelung, W.; Lang, F.; Kuzyakov, Y.; Feger, K. H.; Gottselig, N.; Klumpp, E.; Missong, A.; Winkelmann, C.; Uhlig, D.; Sohrt, J.; von Wilpert, K.; Wu, B.; Hagedorn, F. Dissolved and Colloidal Phosphorus Fluxes in Forest Ecosystems—an Almost Blind Spot in Ecosystem Research. *J. Plant Nutr. Soil Sci.* **2016**, *179* (4), 425–438. https://doi.org/10.1002/jpln.201600079.

(17) Liang, X.; Jin, Y.; Zhao, Y.; Wang, Z.; Yin, R.; Tian, G. Release and Migration of Colloidal Phosphorus from a Typical Agricultural Field under Long-Term Phosphorus Fertilization in Southeastern China. *J. Soils Sediments* **2016**, *16* (3), 842–853. https://doi.org/10.1007/s11368-015-1290-4.

(18) Zarafshar, M.; Bazot, S.; Matinizadeh, M.; Bordbar, S. K.; Rousta, M. J.; Kooch, Y.; Enayati, K.; Abbasi, A.; Negahdarsaber, M. Do Tree Plantations or Cultivated Fields Have the Same Ability to Maintain Soil Quality as Natural Forests? *Appl. Soil Ecol.* **2020**, *151*, 103536. https://doi.org/10.1016/j.apsoil.2020.103536.

(19) Jiang, X.; Bol, R.; Nischwitz, V.; Siebers, N.; Willbold, S.; Vereecken, H.; Amelung, W.; Klumpp, E. Phosphorus Containing Water Dispersible Nanoparticles in Arable Soil. *J. Environ. Qual.* **2015**, *44* (6), 1772–1781. https://doi.org/10.2134/jeq2015.02.0085.

(20) Missong, A.; Bol, R.; Nischwitz, V.; Krüger, J.; Lang, F.; Siemens, J.; Klumpp, E. Phosphorus

in Water Dispersible-Colloids of Forest Soil Profiles. *Plant Soil* **2018**, *427* (1–2), 71–86. https://doi.org/10.1007/s11104-017-3430-7.

(21) Gu, S.; Gruau, G.; Dupas, R.; Jeanneau, L. Evidence of Colloids as Important Phosphorus Carriers in Natural Soil and Stream Waters in an Agricultural Catchment. *J. Environ. Qual.* **2020**, *49* (4), 921–932. https://doi.org/10.1002/jeq2.20090.

(22) Jiang, X.; Bol, R.; Cade-Menun, B. J.; Nischwitz, V.; Willbold, S.; Bauke, S.; Vereecken, H.; Amelung, W.; Klumpp, E. Colloid-Bound and Dissolved Phosphorus Species in Topsoil Water Extracts along a Grassland Transect from Cambisol to Stagnosol. *Biogeosciences* **2017**, *14* (5), 1153–1164. https://doi.org/10.5194/bg-14-1153-2017.

(23) Giddings, J. C.; Yang, F. J. F.; Myers, M. N. Flow Field-Flow Fractionation: A Versatile New Separation Method. *Science (80-.).* **1976**, *193* (4259), 1244–1245. https://doi.org/10.1126/science.959835.

(24) Gottselig, N.; Amelung, W.; Kirchner, J. W.; Bol, R.; Eugster, W.; Granger, S. J.; Hernández-Crespo, C.; Herrmann, F.; Keizer, J. J.; Korkiakoski, M.; Laudon, H.; Lehner, I.; Löfgren, S.; Lohila, A.; Macleod, C. J. A.; Mölder, M.; Müller, C.; Nasta, P.; Nischwitz, V.; Paul-Limoges, E.; Pierret, M. C.; Pilegaard, K.; Romano, N.; Sebastià, M. T.; Stähli, M.; Voltz, M.; Vereecken, H.; Siemens, J.; Klumpp, E. Elemental Composition of Natural Nanoparticles and Fine Colloids in European Forest Stream Waters and Their Role as Phosphorus Carriers. *Global Biogeochem. Cycles* **2017**, *31* (10), 1592–1607. https://doi.org/10.1002/2017GB005657.

(25) Jiang, X.; Bol, R.; Willbold, S.; Vereecken, H.; Klumpp, E. Speciation and Distribution of P

Associated with Fe and Al Oxides in Aggregate-Sized Fraction of an Arable Soil. *Biogeosciences* **2015**, *12* (21), 6443–6452. https://doi.org/10.5194/bg-12-6443-2015.

(26) Missong, A.; Holzmann, S.; Bol, R.; Nischwitz, V.; Puhlmann, H.; v. Wilpert, K.; Siemens, J.; Klumpp, E. Leaching of Natural Colloids from Forest Topsoils and Their Relevance for Phosphorus Mobility. *Sci. Total Environ.* **2018**, *634*, 305–315. https://doi.org/10.1016/j.scitotenv.2018.03.265.

(27) Liu, X. P.; Bi, Q. F.; Qiu, L. L.; Li, K. J.; Yang, X. R.; Lin, X. Y. Increased Risk of Phosphorus and Metal Leaching from Paddy Soils after Excessive Manure Application: Insights from a Mesocosm Study. *Sci. Total Environ.* **2019**, *666*, 778–785. https://doi.org/10.1016/j.scitotenv.2019.02.072.

(28) Weyers, E.; Strawn, D. G.; Peak, D.; Baker, L. L. Inhibition of Phosphorus Sorption on Calcite by Dairy Manure-Sourced DOC. *Chemosphere* **2017**, *184*, 99–105. https://doi.org/10.1016/j.chemosphere.2017.05.141.

(29) Niyungeko, C.; Liang, X.; Liu, C.; Liu, Z. wen; Sheteiwy, M.; Zhang, H.; Zhou, J.; Tian, G. Effect of Biogas Slurry Application Rate on Colloidal Phosphorus Leaching in Paddy Soil: A Column Study. *Geoderma* **2018**, *325*, 117–124. https://doi.org/10.1016/j.geoderma.2018.03.036.

(30) Niyungeko, C.; Liang, X.; Liu, C.; Zhou, J.; Chen, L.; Lu, Y.; Tiimub, B. M.; Li, F. Effect of Biogas Slurry Application on Soil Nutrients, Phosphomonoesterase Activities, and Phosphorus Species Distribution. *J. Soils Sediments* **2020**, *20* (2), 900–910. https://doi.org/10.1007/s11368-019-02435-y.

(31) Kim, J. A.; Vijayaraghavan, K.; Reddy, D. H. K.; Yun, Y. S. A Phosphorus-Enriched Biochar Fertilizer from Bio-Fermentation Waste: A Potential Alternative Source for Phosphorus Fertilizers. *J. Clean. Prod.* **2018**, *196*, 163–171. https://doi.org/10.1016/j.jclepro.2018.06.004.

(32) Hosseini, S. H.; Liang, X.; Niyungeko, C.; Miaomiao, H.; Li, F.; Khan, S.; Eltohamy, K. M. Effect of Sheep Manure-Derived Biochar on Colloidal Phosphorus Release in Soils from Various Land Uses. *Environ. Sci. Pollut. Res.* **2019**, *26* (36), 36367–36379. https://doi.org/10.1007/s11356-019-06762-y.

(33) Li, F. Y.; Liang, X. Q.; Niyungeko, C.; Sun, T.; Liu, F.; Arai, Y. Effects of Biochar Amendments on Soil Phosphorus Transformation in Agricultural Soils. *Adv. Agron.* **2019**, *158*, 131–172. https://doi.org/10.1016/bs.agron.2019.07.002.

(34) Zhang, H.; Chen, C.; Gray, E. M.; Boyd, S. E.; Yang, H.; Zhang, D. Roles of Biochar in Improving Phosphorus Availability in Soils: A Phosphate Adsorbent and a Source of Available Phosphorus. *Geoderma* **2016**, *276*, 1–6. https://doi.org/10.1016/j.geoderma.2016.04.020.

(35) Wang, S.; Li, T.; Zheng, Z. Distribution of Microbial Biomass and Activity within Soil Aggregates as Affected by Tea Plantation Age. *Catena* **2017**, *153*, 1–8. https://doi.org/10.1016/j.catena.2017.01.029.

(36) ISO11277. *Soil Quality – Determination of Particle Size Distribution in Mineral Soil Material – Method by Sieving and Sedimentation*; International Organization for Standarization: Geneva, Switzerland, 1998.

(37) Sumner, M. E.; Miller, W. P. Cation Exchange Capacity and Exchange Coefficients. *Methods*

543 *Soil Anal. Part 3 Chem. Methods* **2018**, 1201–1229.
544 https://doi.org/10.2136/sssabookser5.3.c40.
545 (38) Walker, T. W.; Adams, A. F. R. Studies on Soil Organic Matter: I. Influence of Phosphorus
546 Content of Parent Materials on Accumulations of Carbon, Nitrogen, Sulfur, and Organic
547 Phosphorus in Grassland Soils. *Soil Sci.* **1958**, *85* (6), 307–318.
548 https://doi.org/10.1097/00010694-195806000-00004.
549 (39) Schwertmann, U. The Differenciation of Iron Oxides in Soils by Extraction with NH4-
550 Oxalates Solution. *Zeitschrift für Pflanzenernährung und Bodenkd.* **1964**, *105*, 194–202.
551 (40) Olsen, S. R.; Sommers, L. E. Phosphorus. In *Methods of Soil Analysis Part 2 Chemical and*
552 *Microbiological Properties*; Page, A. L., Ed.; American Society of Agronomy, Soil Science
553 Society of America: Madison, 1982; pp 403–430.
554 (41) Séquaris, J. M.; Lewandowski, H. Physicochemical Characterization of Potential Colloids
555 from Agricultural Topsoils. In *Colloids and Surfaces A: Physicochemical and Engineering*
556 *Aspects*; 2003; Vol. 217, pp 93–99. https://doi.org/10.1016/S0927-7757(02)00563-0.
557 (42) Wang, L.; Missong, A.; Amelung, W.; Willbold, S.; Prietzel, J.; Klumpp, E. Dissolved and
558 Colloidal Phosphorus Affect P Cycling in Calcareous Forest Soils. *Geoderma* **2020**, *375*,
559 114507. https://doi.org/10.1016/j.geoderma.2020.114507.
560 (43) Moradi, G.; Bol, R.; Trbojevic, L.; Missong, A.; Mörchen, R.; Fuentes, B.; May, S. M.;
561 Lehndorff, E.; Klumpp, E. Contrasting Depth Distribution of Colloid-Associated Phosphorus
562 in the Active and Abandoned Sections of an Alluvial Fan in a Hyper-Arid Region of the
563 Atacama Desert. *Glob. Planet. Change* **2020**, *185*, 114170.

https://doi.org/10.1016/j.gloplacha.2019.103090.

(44) Hathaway, J. C. Procedure for Clay Mineral Analyses Used in the Sedimentary Petrology Laboratory of the U.S. Geological Survey*. *Clay Miner.* **1956**, *3* (15), 8–13. https://doi.org/10.1180/claymin.1956.003.15.05.

(45) Nischwitz, V.; Goenaga-Infante, H. Improved Sample Preparation and Quality Control for the Characterisation of Titanium Dioxide Nanoparticles in Sunscreens Using Flow Field Flow Fractionation On-Line with Inductively Coupled Plasma Mass Spectrometry. *J. Anal. At. Spectrom.* **2012**, *27* (7), 1084–1092. https://doi.org/10.1039/c2ja10387g.

(46) Nischwitz, V.; Gottselig, N.; Missong, A.; Meyn, T.; Klumpp, E. Field Flow Fractionation Online with ICP-MS as Novel Approach for the Quantification of Fine Particulate Carbon in Stream Water Samples and Soil Extracts. *J. Anal. At. Spectrom.* **2016**, *31* (9), 1858–1868. https://doi.org/10.1039/c6ja00027d.

(47) Zang, L.; Tian, G. M.; Liang, X. Q.; He, M. M.; Bao, Q. B.; Yao, J. H. Profile Distributions of Dissolved and Colloidal Phosphorus as Affected by Degree of Phosphorus Saturation in Paddy Soil. *Pedosphere* **2013**, *23* (1), 128–136. https://doi.org/10.1016/S1002-0160(12)60088-5.

(48) Audette, Y.; Smith, D. S.; Parsons, C. T.; Chen, W.; Rezanezhad, F.; Van Cappellen, P. Phosphorus Binding to Soil Organic Matter via Ternary Complexes with Calcium. *Chemosphere* **2020**, *260*, 127624. https://doi.org/10.1016/j.chemosphere.2020.127624.

(49) Elliott, J. C. Structure and Chemistry of the Apatites and Other Calcium Orthophosphates. *Stud. Org. Chem.* **1994**, *18*, 94008066–94008066.

(50) Fu, B.; Sun, X.; Qian, W.; Shen, Y.; Chen, R.; Hannig, M. Evidence of Chemical Bonding to Hydroxyapatite by Phosphoric Acid Esters. *Biomaterials* **2005**, *26* (25), 5104–5110. https://doi.org/10.1016/j.biomaterials.2005.01.035.

(51) Lin, J.; Zhang, Z.; Zhan, Y. Effect of Humic Acid Preloading on Phosphate Adsorption onto Zirconium-Modified Zeolite. *Environ. Sci. Pollut. Res.* **2017**, *24* (13), 12195–12211. https://doi.org/10.1007/s11356-017-8873-0.

(52) Yang, X.; Chen, X.; Yang, X. Effect of Organic Matter on Phosphorus Adsorption and Desorption in a Black Soil from Northeast China. *Soil Tillage Res.* **2019**, *187*, 85–91. https://doi.org/10.1016/j.still.2018.11.016.

(53) Said-Pullicino, D.; Giannetta, B.; Demeglio, B.; Missong, A.; Gottselig, N.; Romani, M.; Bol, R.; Klumpp, E.; Celi, L. Redox-Driven Changes in Water-Dispersible Colloids and Their Role in Carbon Cycling in Hydromorphic Soils. *Geoderma* **2021**, *385*, 114894. https://doi.org/10.1016/j.geoderma.2020.114894.

(54) Regelink, I. C.; Weng, L.; Koopmans, G. F.; van Riemsdijk, W. H. Asymmetric Flow Field-Flow Fractionation as a New Approach to Analyse Iron-(Hydr)Oxide Nanoparticles in Soil Extracts. *Geoderma* **2013**, *202–203*, 134–141. https://doi.org/10.1016/j.geoderma.2013.03.015.

(55) Lazaratou, C. V.; Vayenas, D. V.; Papoulis, D. The Role of Clays, Clay Minerals and Clay-Based Materials for Nitrate Removal from Water Systems: A Review. *Appl. Clay Sci.* **2020**, *185*, 105377. https://doi.org/10.1016/j.clay.2019.105377.

(56) Zhejiang Soil Census Office. *Soil of Zhejiang*; Zhejiang Science and Technology Press:

606 Hangzhou, 1994.
607 (57) Kéri, A.; Dähn, R.; Marques Fernandes, M.; Scheinost, A. C.; Krack, M.; Churakov, S. V.
608 Iron Adsorption on Clays Inferred from Atomistic Simulations and X-Ray Absorption
609 Spectroscopy. *Environ. Sci. Technol.* **2020**, *54* (19), 11886–11893.
610 https://doi.org/10.1021/acs.est.9b07962.
611 (58) Laegdsmand, M.; De Jonge, L. W.; Moldrup, P. Leaching of Colloids and Dissolved Organic
612 Matter from Columns Packed with Natural Soil Aggregates. *Soil Sci.* **2005**, *170* (1), 13–27.
613 https://doi.org/10.1097/00010694-200501000-00003.
614 (59) Laegdsmand, M.; Moldrup, P.; De Jonge, L. W. Modelling of Colloid Leaching from
615 Unsaturated, Aggregated Soil. *Eur. J. Soil Sci.* **2007**, *58* (3), 692–703.
616 https://doi.org/10.1111/j.1365-2389.2006.00854.x.
617 (60) Bhatti, J. S.; Comerford, N. B.; Johnston, C. T. Influence of Oxalate and Soil Organic Matter
618 on Sorption and Desorption of Phosphate onto a Spodic Horizon. *Soil Sci. Soc. Am. J.* **1998**,
619 *62* (4), 1089–1095. https://doi.org/10.2136/sssaj1998.03615995006200040033x.
620 (61) Yaghi, N.; Hartikainen, H. Enhancement of Phosphorus Sorption onto Light Expanded Clay
621 Aggregates by Means of Aluminum and Iron Oxide Coatings. *Chemosphere* **2013**, *93* (9),
622 1879–1886. https://doi.org/10.1016/j.chemosphere.2013.06.059.
623 (62) Holzmann, S.; Missong, A.; Puhlmann, H.; Siemens, J.; Bol, R.; Klumpp, E.; Wilpert, K. von.
624 Impact of Anthropogenic Induced Nitrogen Input and Liming on Phosphorus Leaching in
625 Forest Soils. *J. Plant Nutr. Soil Sci.* **2016**, *179* (4), 443–453.
626 https://doi.org/10.1002/jpln.201500552.

(63) Celi, L.; Barberis, E. Abiotic Stabilization of Organic Phosphorus in the Environment. In *Organic Phosphorus in the Environment*; Turner, B. L., Frossard, E., Baldwin, D. S., Eds.; 2004; pp 113–132. https://doi.org/10.1079/9780851998220.0113.

(64) Li, F. Y.; Yuan, C. yu; Yuan, Z. Q.; You, Y. jun; Hu, X. fei; Wang, S.; Li, G. yu. Bioavailable Phosphorus Distribution in Alpine Meadow Soil Is Affected by Topography in the Tian Shan Mountains. *J. Mt. Sci.* **2020**, *17* (2), 410–422. https://doi.org/10.1007/s11629-019-5705-3.

(65) Guppy, C. N.; Menzies, N. W.; Moody, P. W.; Blamey, F. P. C. Competitive Sorption Reactions between Phosphorus and Organic Matter in Soil: A Review. *Australian Journal of Soil Research*. 2005, pp 189–202. https://doi.org/10.1071/SR04049.

(66) Hou, E.; Chen, C.; Wen, D.; Liu, X. Relationships of Phosphorus Fractions to Organic Carbon Content in Surface Soils in Mature Subtropical Forests, Dinghushan, China. *Soil Res.* **2014**, *52* (1), 55–63. https://doi.org/10.1071/SR13204.

(67) Spohn, M. Increasing the Organic Carbon Stocks in Mineral Soils Sequesters Large Amounts of Phosphorus. *Glob. Chang. Biol.* **2020**, *26* (8), 4169–4177. https://doi.org/10.1111/gcb.15154.

(68) Sato, S.; Solomon, D.; Hyland, C.; Ketterings, Q. M.; Lehmann, J. Phosphorus Speciation in Manure and Manure-Amended Soils Using XANES Spectroscopy. *Environ. Sci. Technol.* **2005**, *39* (19), 7485–7491. https://doi.org/10.1021/es0503130.

(69) Zhou, J.; Liang, X.; Shan, S.; Yan, D.; Chen, Y.; Yang, C.; Lu, Y.; Niyungeko, C.; Tian, G. Nutrient Retention by Different Substrates from an Improved Low Impact Development System. *J. Environ. Manage.* **2019**, *238*, 331–340.

https://doi.org/10.1016/j.jenvman.2019.03.019.

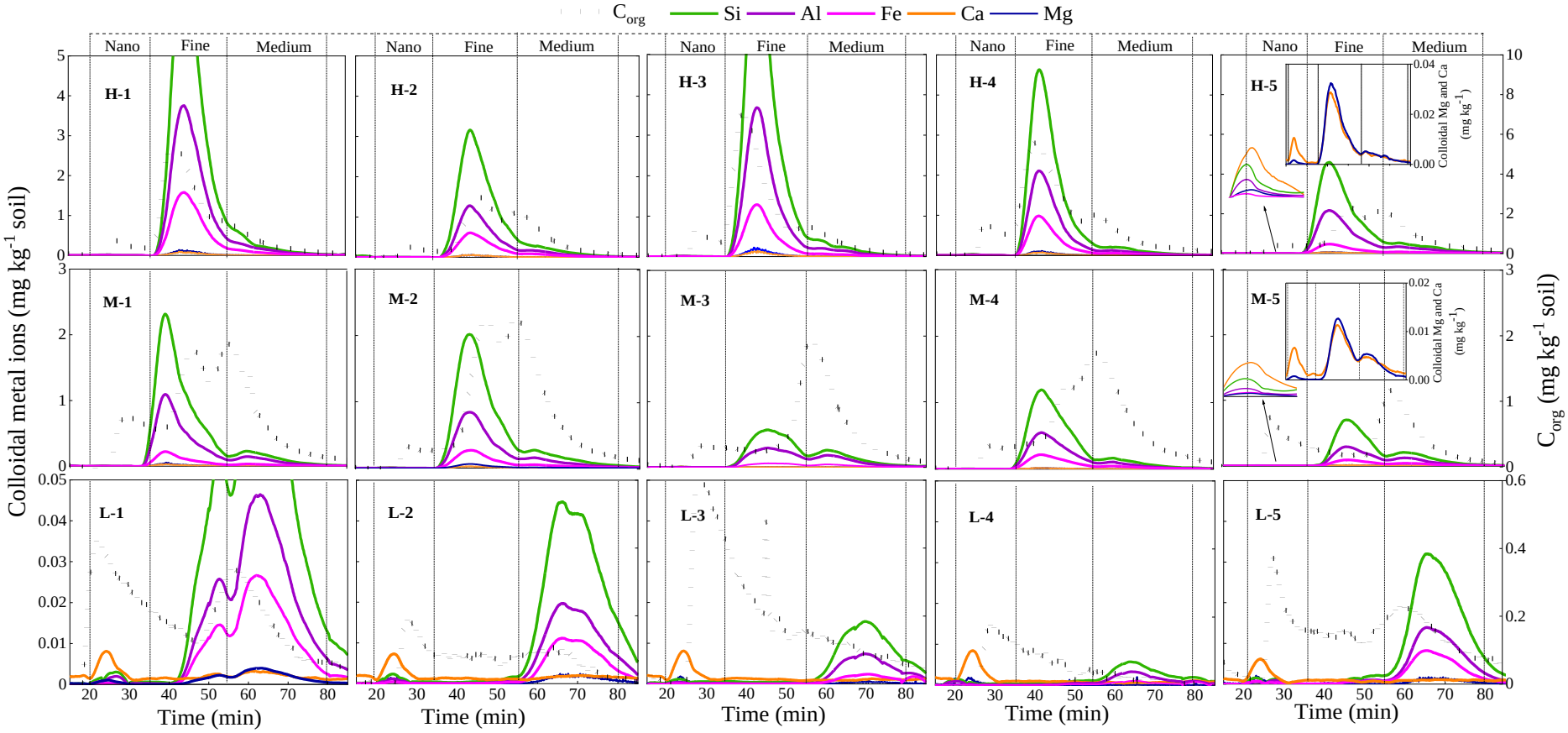

Figure 1. The fractogram of colloidal elements such as aluminum (Al), iron (Fe), silicon (Si), calcium (Ca), and organic carbon (C_{org}) in the soils at 15 sites by Asymmetrical Flow Field Flow Fractionation (AF4) coupled with Inductively Coupled Plasma-Mass Spectrometer (ICP-MS) and Organic Carbon Detector (OCD). "Nano" is nano colloidal fraction (0.6–25 nm); "Fine" is fine colloidal fraction (25–160 nm); "Medium" is medium colloidal fraction (160–500 nm).

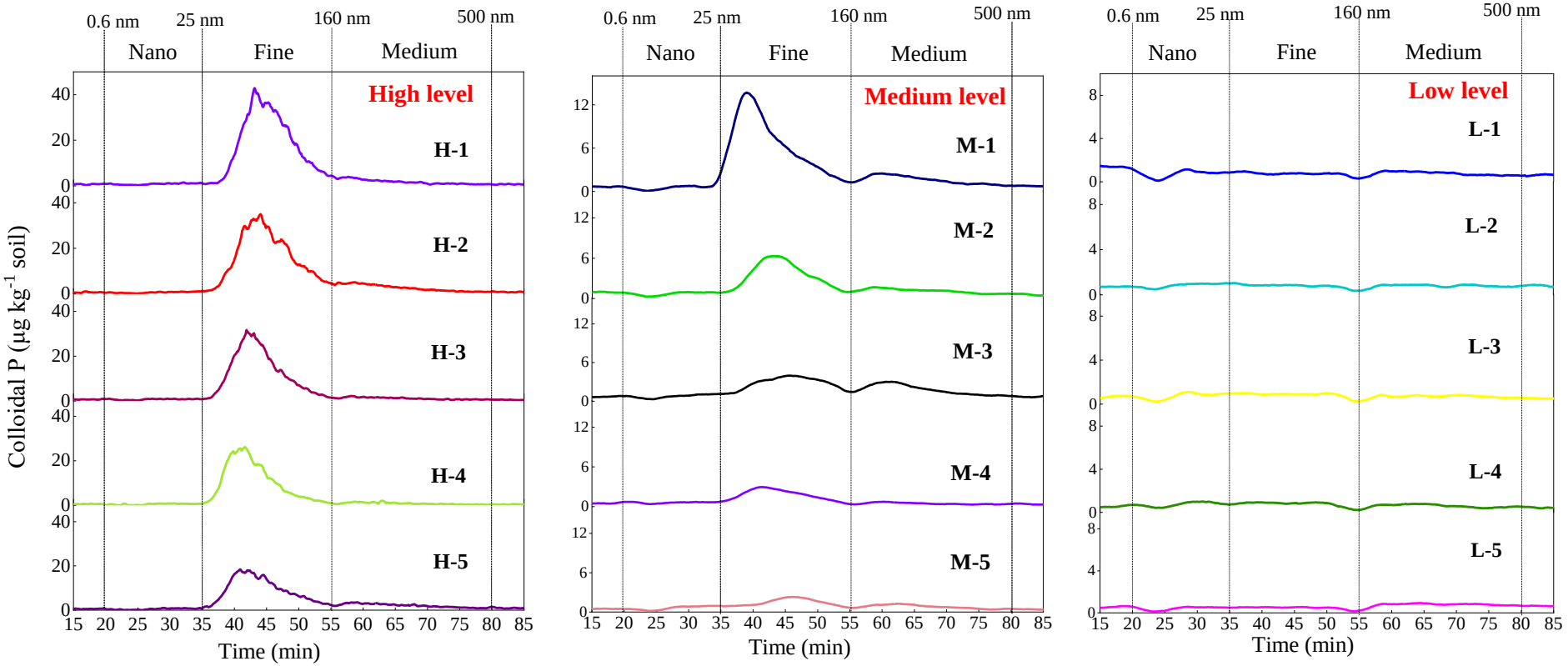

Figure 2. The fractogram of nano-colloidal (Nano), fine-colloidal (Fine) and medium-colloidal (Medium) phosphorus (P) in the 15 soils measured by Asymmetrical Flow Field Flow Fractionation (AF4) coupled with Inductively Coupled Plasma-Mass Spectrometer (ICP-MS). High, medium, and low levels indicate the peak level of colloidal P in the soils. Y-axis are scaled differently for the three figures.

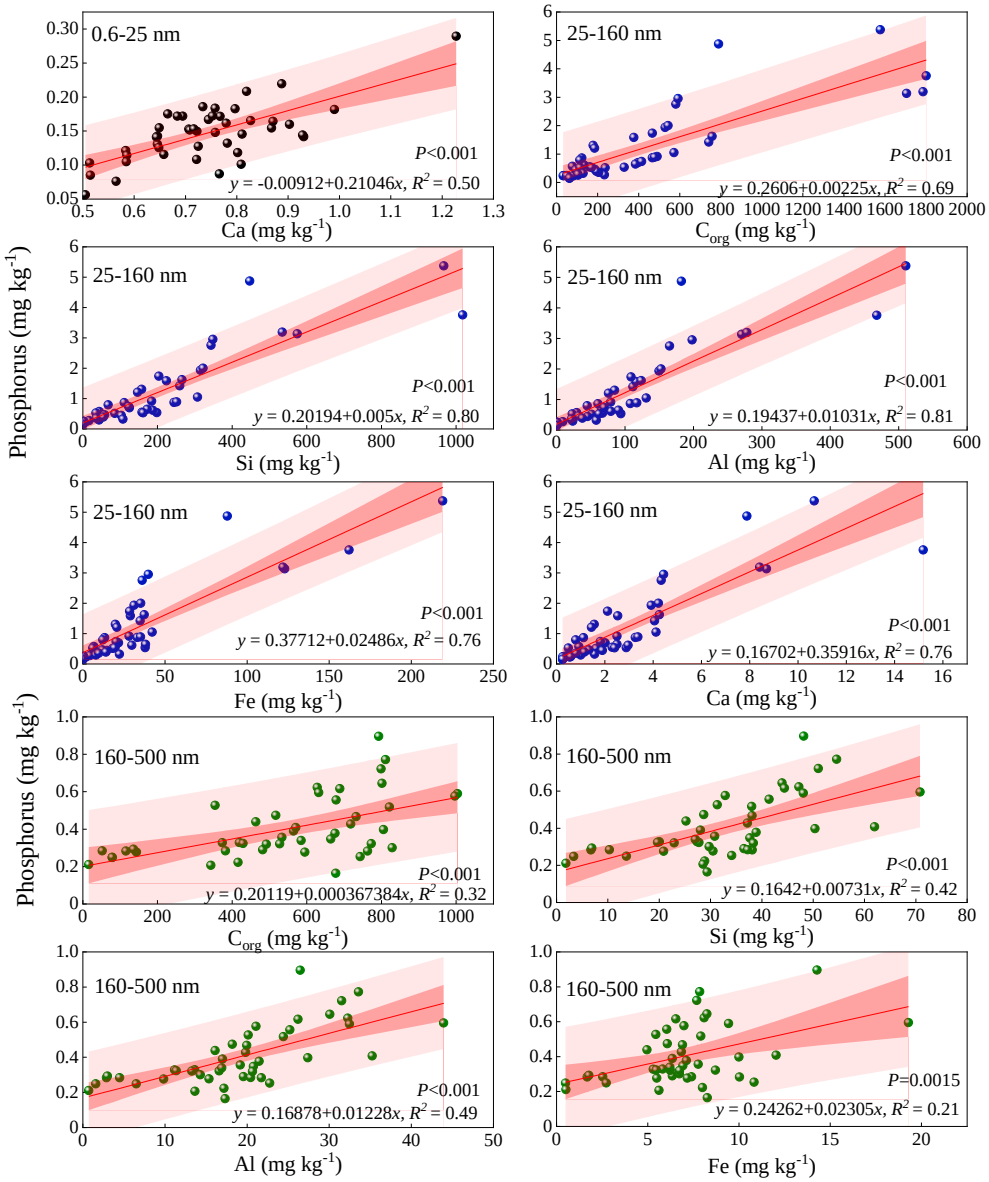

Figure 3. Nano- (0.6–25 nm), fine- (25–160 nm) and medium- (160–500 nm) colloidal phosphorus as a function of the content of other components in the same particle size fractions such as organic carbon (C_{org}), silicon (Si), aluminum (Al), iron (Fe), and calcium (Ca) (n=45)

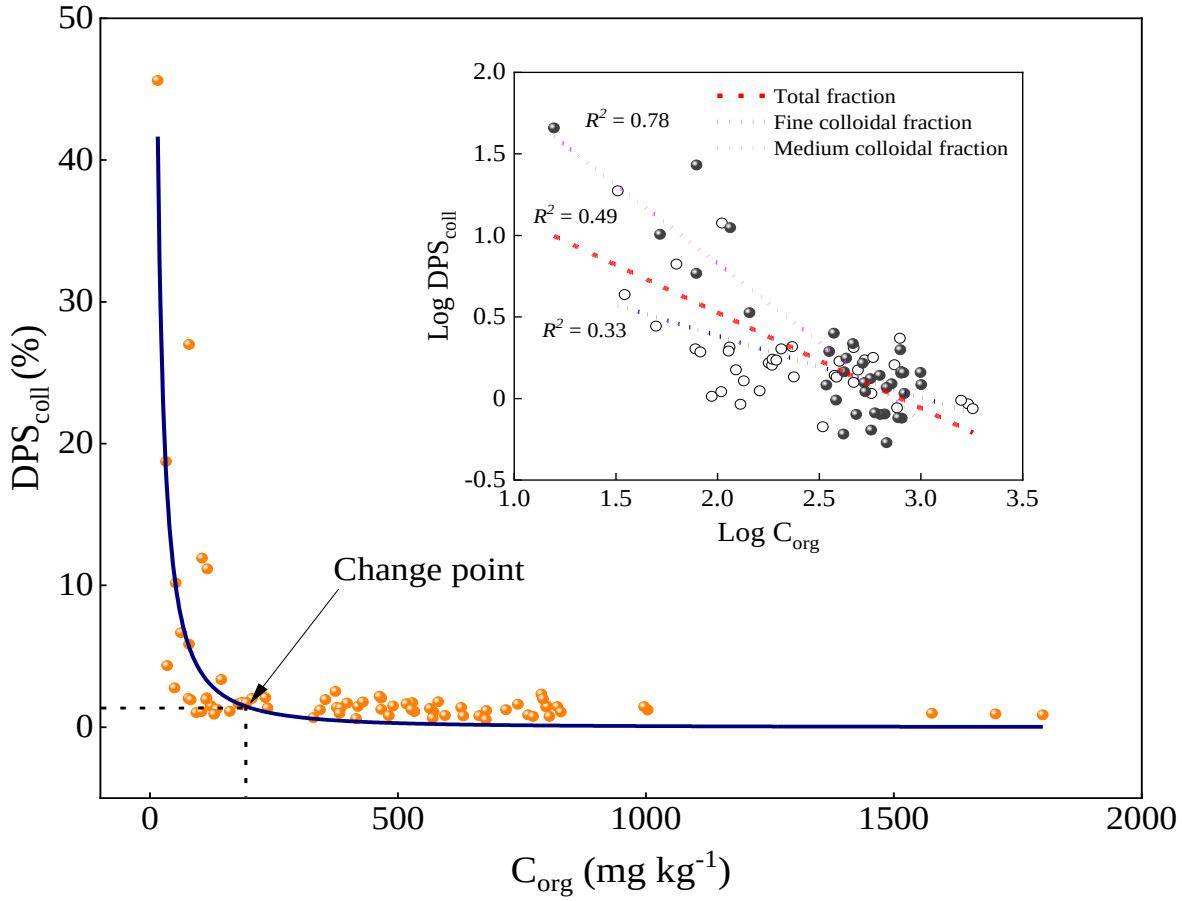

Figure 4. The relationship between colloidal phosphorus saturation (DPS_{coll}) and colloidal organic carbon (C_{org}) (a), and the related linear fitting plot of DPS_{coll} and C_{org} after Log transformation (b).

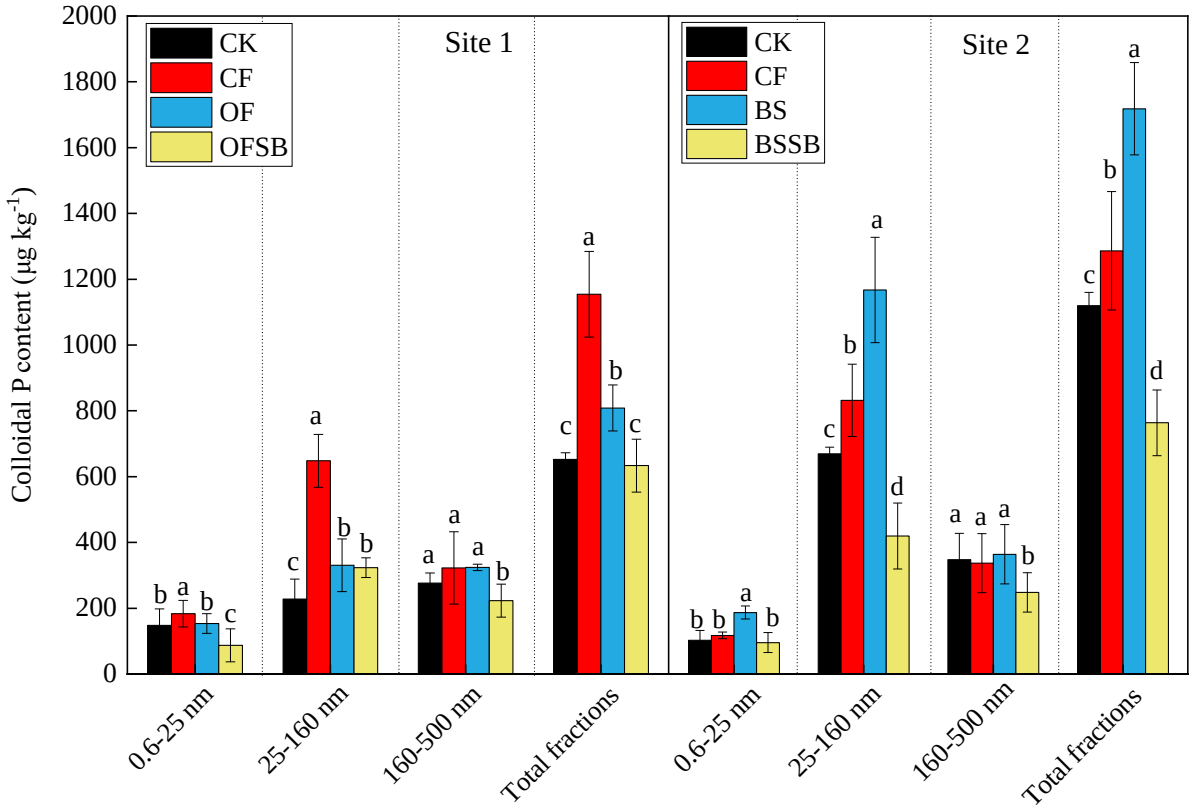

Figure 5. Nano-, fine- and medium-colloidal phosphorus (P) content of different fractions in the soils at Site 1 and Site 2 under different fertilization treatments (n=3). CK represents control without fertilizer; CF represents conventional fertilization (chemical fertilizer); OF or BS represents organic fertilizer (sheep manure) or biogas slurry instead of 30% P application rate of chemical fertilizer, respectively; OFSB or BSSB represents organic fertilizer or biogas slurry + modified rice straw biochar instead of 30% P application rate of chemical fertilizer, respectively; Lowercase indicated significant difference between different fertilization treatments at $P < 0.05$ level.

677 **Table 1.** Colloidal phosphorus content and saturation (DPS_{coll}) of different particle size fractions in the 15 representative soils with different
678 land-use types in Zhejiang Province, China.

Soils	Colloidal P content (μg kg^{-1})				DPS_{coll} (%)		
	0.6–25 nm	25–160 nm	160–500 nm	Sum of fractions	25–160 nm	160–500 nm	Sum of fractions
H-1	172±11	5375±195	595±67	6142±214	0.8±0.1	1.0±0.1	0.8±0.2
H-2	142±25	4874±368	896±77	5912±359	1.9±0.3	2.4±0.1	2.0±0.2
H-3	155±13	3756±411	408±37	4318±498	0.6±0.1	0.9±0.1	0.6±0.3
H-4	103±9.0	3135±165	283±33	3603±189	0.8±0.1	0.9±0.1	0.9±0.2
H-5	108±10	2753±123	722±92	3583±189	1.3±0.0	2.0±0.1	1.4±0.2
M-1	121±11	1935±110	556±149	2612±99	1.0±0.1	1.7±0.2	1.2±0.1
M-2	150±24	1050±127	397±45	1597±145	0.6±0.0	1.1±0.3	0.8±0.2
M-3	160±29	863±102	623±77	1646±212	1.1±0.2	1.5±0.2	1.4±0.3
M-4	126±14	534±46	164±28	824±56	0.4±0.2	0.7±0.1	0.5±0.1
M-5	131±20	444±44	284±29	859±89	0.7±0.2	1.0±0.1	1.0±0.2
L-1	148±25	228±21	277±31	653±68	4.7±1.0	2.0±0.6	3.4±0.1
L-2	172±36	242±20	284±20	697±77	125±14	4.3±0.2	10±1.5
L-3	151±10	258±20	248±13	658±51	88±14	12±2.3	27±4.3
L-4	153±8.2	236±11	211±22	601±40	150±21	19±3.1	46±7.2
L-5	85±7.1	146±26	283±44	514±68	60±5.5	6.6±1.1	11±2.1

679

680

681 **Table 2.** The average (n=3) content of colloidal aluminum (Al), iron (Fe), silicon (Si), calcium (Ca), and organic carbon (C_{org}) content in
682 the nano- (0.6–25 nm), fine- (25–160 nm), and medium- (160–500 nm) colloidal fractions of 15 soils determined by AF4-ICP-MS and
683 AF4-OCD.

Sites	0.6–25 nm (mg kg^{-1})						25–160 nm (mg kg^{-1})						160–500 nm (mg kg^{-1})					
	C_{org}	Mg	Al	Si	Ca	Fe	C_{org}	Mg	Al	Si	Ca	Fe	C_{org}	Mg	Al	Si	Ca	Fe
H-1	166	0.10	0.75	1.2	0.69	0.31	1577	15	510	967	11	219	632	1.3	44	71	1.3	19
H-2	126	0.10	0.30	0.65	0.65	0.13	790	7.5	183	447	7.9	88	793	1.2	26	48	1.5	14
H-3	422	0.10	0.78	1.3	0.87	0.25	1800	23	468	1018	15	162	570	1.6	35	62	1.6	12
H-4	461	0.17	1.4	2.4	0.51	0.59	1705	12	271	574	8.7	123	763	1.0	22	38	1.0	10
H-5	123	0.09	0.24	0.49	0.72	0.06	582	4.9	165	343	4.3	36	799	1.0	32	51	1.0	7.7
M-1	218	0.14	1.7	3.1	0.58	0.42	529	5.5	150	315	3.9	31	679	1.0	25	41	0.77	6.0
M-2	97	0.08	0.20	0.46	0.72	0.07	572	9.2	131	307	4.1	42	806	2.0	27	50	1.0	10
M-3	92	0.12	0.15	0.31	0.90	0.04	123	1.1	61	111	1.1	13	628	0.7	32	47	0.78	8.1
M-4	103	0.07	0.30	0.57	0.65	0.12	330	2.9	94	198	2.9	38	679	0.62	17	29	0.84	8.3
M-5	161	0.07	0.15	0.36	0.65	0.06	94	2.0	45	103	1.9	15	382	1.0	20	37	1.1	7.4
L-1	112	0.08	0.16	0.29	0.76	0.04	82	0.30	3.3	7.4	0.55	1.9	144	0.83	9.9	21	0.79	5.5
L-2	42	0.07	0.09	0.21	0.68	0.04	35	0.02	0.14	0.36	0.38	0.06	52	0.46	4.5	10	0.57	2.5
L-3	165	0.09	0.04	0.15	0.71	0.02	105	0.03	0.24	0.45	0.37	0.04	80	0.11	1.6	3.4	0.36	0.50
L-4	44	0.09	0.02	0.09	0.72	0.01	32	0.01	0.12	0.29	0.26	0.04	16	0.02	0.73	1.8	0.24	0.52
L-5	78	0.09	0.06	0.12	0.51	0.07	63	0.03	0.15	0.30	0.25	0.13	116	0.28	2.9	6.7	0.34	1.7

684

685